Protective effects of safranal on hypoxia/reoxygenation-induced injury in H9c2 cardiac myoblasts via the PI3K/AKT/GSK3β signaling pathway

HEFEI WANG[1*], BIN ZHENG[2*], KAIMENG CHE[1], XUE HAN[1], LI LI[3], HONGFANG WANG[2], YANSHUANG LIU[4], JING SHI[5] and SHIJIANG SUN[6]

[1]Department of Traditional Chinese Medicine and Medical History Literature, School of Basic Medicine; [2]Department of Traditional Chinese Medicine, School of Pharmacy, Hebei University of Chinese Medicine; [3]Department of Pharmacognosy, School of Pharmacy, Hebei Medical University; [4]Department of Diagnostics, Hebei Key Laboratory of Integrative Medicine on Liver-Kidney Patterns, Institute of Integrative Medicine, College of Integrative Medicine, Hebei University of Chinese Medicine, Shijiazhuang, Hebei 050200; [5]Department of Scientific Research Management, The Fourth Hospital of Hebei Medical University, Shijiazhuang, Hebei 050011; [6]Department of Hospital Management and Medical History Literature, Hebei Province Hospital of Chinese Medicine, The First Affiliated Hospital, Hebei University of Chinese Medicine, Shijiazhuang, Hebei 050200, P.R. China

Received May 13, 2021; Accepted September 14, 2021

DOI: 10.3892/etm.2021.10836

Abstract. Safranal (SFR), an active ingredient extracted from saffron, exhibits a protective effect on the cardiovascular system. However, the mechanism of SFR against hypoxia/reoxygenation (H/R)-induced cardiomyocyte injury has previously not been investigated *in vitro*. The aim of the present study was therefore to observe the protective effects of SFR on H/R-induced cardiomyocyte injury and to explore its mechanisms. A H/R injury model of H9c2 cardiac myoblasts was established by administering 800 μmol/l $CoCl_2$ to H9c2 cells for 24 h and reoxygenating the cells for 4 h to induce hypoxia. H9c2 cardiac myoblasts were pretreated with SFR for 12 h to evaluate the associated protective effects. A Cell Counting Kit-8 assay was used for cell viability detection, and the expression levels of lactate dehydrogenase (LDH), creatine kinase-MB (CK-MB), glutathione peroxidase (GSH-px), catalase (CAT), superoxide dismutase (SOD), malondialdehyde (MDA) and caspase-3, and the intracellular Ca^{2+} concentration were measured using the corresponding commercial kits. Levels of reactive oxygen species (ROS) in the cells were detected using 2,7-dichlorodihydrofluorescein diacetate. Flow cytometry was used to determine the degree of apoptosis and the level of mitochondrial membrane potential (MMP). Moreover, the expression levels of phosphorylated (p-)PI3K, AKT, p-AKT, glycogen synthase kinase 3β (GSK3β), p-GSK3β, Bcl-2, Bax, caspase-3 and cleaved caspase-3 were measured using western blot analysis. Results of the present study demonstrated that the H9c2 cardiac myoblasts treated with SFR exhibited significantly improved levels of viability and significantly reduced levels of ROS, compared with the H/R group. Furthermore, compared with the H/R group, SFR treatment significantly increased the MMP levels and antioxidant enzyme levels, including CAT, SOD and GSH-px; whereas the levels of CK-MB, LDH, MDA and intracellular Ca^{2+} concentration were significantly decreased. Moreover, the results of the present study demonstrated that SFR significantly reduced caspase-3, cleaved caspase-3 and Bax protein expression levels, but upregulated the Bcl-2 protein expression levels. SFR also increased the protein expressions of PI3K/AKT/GSK3β. In summary, the results suggested that SFR may exert a protective effect against H/R-induced cardiomyocyte injury, which occurs in connection with the inhibition of oxidative stress and apoptosis via regulation of the PI3K/AKT/GSK3β signaling pathway.

Correspondence to: Professor Jing Shi, Department of Scientific Research Management, The Fourth Hospital of Hebei Medical University, 12 Jiankang Road, Shijiazhuang, Hebei 050011, P.R. China
E-mail: 13931143718@139.com

Professor Shijiang Sun, Department of Hospital Management and Medical History Literature, Hebei Province Hospital of Chinese Medicine, The First Affiliated Hospital, Hebei University of Chinese Medicine, 389 Zhongshan East Road, Changan, Shijiazhuang, Hebei 050200, P.R. China
E-mail: sunshijiang6909@163.com

*Contributed equally

Key words: safranal, H9c2 cardiac myoblasts, anti-oxidant stress, hypoxia/reoxygenation, anti-apoptosis, PI3K/AKT/GSK3β signaling pathway

Introduction

Since 1990, the global cardiovascular disease (CVD) mortality rate has increased annually, with CVD being the leading cause of death worldwide, especially in developing countries (1-3). Acute myocardial infarction (AMI) is a significant contributor

towards high mortality in CVD (4). For patients with AMI, rapid and effective opening of the blocked vessel rescues ischemic myocardium, reduces infarct size and improves the effectiveness of treatment. Reperfusion therapies, such as thrombolysis and percutaneous coronary intervention, are the most effective treatments for AMI (5). However, reperfusion of blood flow brought about by the opening of the culprit vessel causes damage to cardiac myoblasts, which is known as myocardial ischemia/reperfusion injury (MIRI) (6). A previous study demonstrated that the area of myocardial infarction caused by MIRI was 50% of the total area of myocardial infarction (7). Therefore, the attenuation of MIRI and improvements to the efficacy of reperfusion therapies in AMI are major focus areas of research.

The concept of MIRI was first proposed by Jennings (8) in 1960; however, the pathophysiological mechanisms of MIRI are still not completely understood. Currently, the accepted mechanisms for MIRI include oxygen radical generation, intracellular Ca^{2+} ($[Ca^{2+}]_i$) overload and apoptosis (9,10). Moreover, previous studies have confirmed that cardiomyocyte apoptosis is an important pathway and characteristic in MIRI (11,12). During MIRI, mechanisms such as ($[Ca^{2+}]_i$) overload, increases in mitochondrial permeability and excessive accumulation of reactive oxygen species (ROS) can induce cardiomyocyte apoptosis, thereby exacerbating MIRI (13). It is therefore important to identify drugs that can effectively alleviate oxidative stress, reduce ($[Ca^{2+}]_i$) concentration and improve mitochondrial function in MIRI.

During MIRI, the reperfusion injury salvage kinase (RISK) signaling pathway is activated, which includes protein kinase B (AKT) and phosphatidylinositol 3 kinase (PI3K) (14). The PI3K/AKT/glycogen synthase kinase 3β (GSK3β) axis is an intracellular signaling transduction pathway that serves important biological functions in cellular activities, including apoptosis, survival and proliferation (15). PI3K can be phosphorylation-activated by extracellular signals such as growth factors. Activated PI3K further catalyzes the phosphorylation of the 3'-OH position on the inositol ring of phosphatidylinositol 4,5-bisphosphate at the cell membrane surface to form the 3,4,5-triphosphate phosphatidylinositol (PIP3), and PIP3 activates the phosphorylation of AKT as a secondary messenger (16). Phosphorylated AKT can then further phosphorylate GSK3β initiating a cardio-protective mechanism (16). It has been reported that drug pretreatment can activate the PI3K/AKT/GSK3β signaling pathway in cardiomyocytes *in vivo* and *in vitro*, which serves an important role in combating MIRI (17,18). Furthermore, a previous study has demonstrated that ischemic preconditioning can reduce myocardial infarct size following ischemia/reperfusion in mice, during which the level of phosphorylated AKT *in vivo* is significantly increased (19). GSK3β can open the mitochondrial permeability transition pore and promote apoptosis following its activation, whereas inactive phosphorylated GSK3β can shield cardiomyocytes and mitochondria from damage, serving a myocardial protective role (20).

Saffron, which is derived from the dried stigmas of the saffron plant of the Iridaceae family, is native to Europe and is expensive due to its low yield and manual plucking methods (21). Saffron has been used for thousands of years as a dye and as a spice for cooking (22). It is also commonly used in the clinic to treat cardio and cerebrovascular diseases (23,24). Safranal (SFR; C10H14O; Fig. 1) is a major aromatic factor in saffron, accounting for 60-70% of the volatile constituents (25). Studies have previously demonstrated that SFR has numerous pharmacological properties, including as an antioxidant (26), antiapoptotic (27), anticancer (28,29) and cardioprotective factor (30-32). Furthermore, in our previous study, Xue *et al* (33) determined that SFR could inhibit the L-type Ca^{2+} current and cell contractility and improve ischemic myocardial tissue. Results of a previous study demonstrated that the protective effects of SFR against MIRI are associated with the PI3K/AKT/endothelial nitric oxide synthase signaling pathway *in vivo* (32), cardiac function is regulated by a series of factors, including the nervous system and hormones. Therefore, the mechanism of SFR in MIRI needs further investigation at the cellular level.

In the present study, a hypoxia/reoxygenation (H/R) injury model was established by subjecting H9c2 cardiac myoblasts to hypoxia with cobalt chloride ($CoCl_2$) containing medium followed by reoxygenation with normal medium. The protective effects of SFR were evaluated by exploring the H9c2 cardiac myoblast viability, as well as the oxidative stress and apoptotic levels of the cells in the H/R model. Furthermore, the protein expression levels of the PI3K/AKT/GSK3β signaling pathway were explored to elucidate the potential mechanism of SFR. The effect of SFR on intracellular ($[Ca^{2+}]_i$) overload and ROS production was also observed. The present study builds upon the findings of our previous study (33) and provides an experimental and theoretical basis for the clinical application of SFR in the treatment of MIRI.

Materials and methods

Reagents. The SFR (cat. no. S081900) and $CoCl_2$ (cat. no. C633133) used in the present study was purchased from Toronto Research Chemicals, Inc. The rat cardiac myoblast H9c2 cell line was obtained from Bluefbio Biotechnology Development, Inc (cat. no. BFN60804388). High glucose Dulbecco's modified eagle medium (DMEM; cat. no. 12430047) and fetal bovine serum (FBS; cat. no. 10093188) were purchased from Gibco (Thermo Fisher Scientific, Inc.). The Cell Counting Kit (CCK)-8 assay (cat. no. G021-1-1), lactate dehydrogenase (LDH) assay (cat. no. A020-2-1), creatine kinase-MB (CK-MB) assay (cat. no. H197-1-1), glutathione peroxidase (GSH-Px) assay (cat. no. A005-1-2), catalase (CAT) assay (cat. no. A007-1-1), superoxide dismutase (SOD) assay (cat. no. A001-3-2), malondialdehyde (MDA) assay (cat. no. A003-1-2), caspase-3 assay (cat. no. G015-1-3), BCA protein assay (cat. no. A045-3-2) and Ca^{2+} assay (cat. no. C004-1-1) were obtained from Nanjing Jiancheng Bioengineering Inc. LY294002, a specific antagonist of PI3K/AKT (cat. no. HY-10108), was purchased from MedChemExpress, Inc. All other reagents used in the present study were purchased from Sigma-Aldrich (Merck KGaA) unless otherwise stated.

Cell culture. H9c2 cells were cultured in the high-glucose DMEM containing 10% FBS and 100 U/ml penicillin/streptomycin. The rat cardiac myoblast H9c2 cell line was initially cultured from rat embryo tissue. The cells grew in a 5% CO_2 incubator at 37˚C and medium was replaced every 2 days.

When cells were ~80% confluent, cells were trypsinized, passaged and seeded into a 96-well or six-well plate. Cells in the logarithmic growth phase were used for further experiments.

H/R model establishment. H9c2 cardiac myoblasts were prepared into $5x10^4$/ml cell suspension and inoculated in a 96-well plate at 100 μl/well. When the cells covered 80% of the wells, different treatments were performed applied according to the needs of the experiment. In the preliminary experiment, 200, 400, 600, 800, 1,000 and 1,200 μmol/l $CoCl_2$ were applied to H9c2 cells and incubated at 37˚C for 24 h. Therefore, the optimal concentration of $CoCl_2$ for hypoxic conditions was determined to be 800 μmol/l. Following hypoxic treatment, high glucose DMEM was used to reoxygenate the cells at 37˚C for 2, 4, 6 and 8 h to establish the optimal reoxygenation time. In summary, the H/R injury model of H9c2 cardiac myoblasts was established by administering 800 μmol/l $CoCl_2$ for 24 h to establish hypoxia prior to reoxygenation for 4 h.

Treatment. All manipulations involving incubation of cells were performed at 37˚C. H9c2 cardiac myoblasts were inoculated in 96-well plates at 5,000 cells/well. H9c2 cardiac myoblasts were randomly divided into the following six groups: i) Control group (CONT), cultured in high-glucose DMEM; ii) H/R injury group (H/R), hypoxia induced cells using 800 μmol/l $CoCl_2$-containing medium for 24 h, followed by reoxygenation with high-glucose DMEM for 4 h; iii) low dose SFR group (SFR_L + H/R), the cells were pretreated with 10 μmol/l of SFR for 12 h, followed by hypoxia induction with 800 μmol/l $CoCl_2$-containing medium for 24 h and reoxygenation with high-glucose DMEM for 4 h; iv) high dose SFR group (SFR_H + H/R), the cells were pretreated with 30 μmol/l of SFR for 12 h, followed by hypoxia induction using 800 μmol/l $CoCl_2$-containing medium for 24 h and reoxygenation with high-glucose DMEM for 4 h; v) high dose SFR alone group (SFR_A), the cells were treated with 30 μmol/l of SFR for 12 h and then cultured in high-glucose DMEM; and vi) antagonist LY294002 group (LY294002 + SFR_H + H/R), the cells were pre-incubated with 20 μmol/l LY294002 for 1 h prior to treatment with 30 μmol/l SFR for 12 h, followed by hypoxia induction using 800 μmol/l $CoCl_2$-containing medium for 24 h and reoxygenation with high-glucose DMEM for 4 h. Furthermore, a preliminary study on the therapeutic effects of post-treatment with SFR was also performed. H9c2 cardiac myoblasts were inoculated into 96-well plates at 5,000 cells/well. H9c2 cardiac myoblasts were randomly divided into the following five groups: i) Control group, high-glucose DMEM culture; ii) H/R injury group, hypoxia was induced using $CoCl_2$ containing medium for 24 h, followed by reoxygenation with high-glucose DMEM for 4 h; iii) low dose SFR group, following H/R treatment, the cells were treated with 10 μmol/l of SFR for 12 h; iv) high dose SFR group, following H/R treatment, the cells were treated with 30 μmol/l of SFR for 12 h; and v) high dose SFR only group, the cells were treated with 30 μmol/l of SFR for 12 h and then cultured in high-glucose DMEM.

Cell viability assay. H9c2 cardiac myoblasts in the logarithmic growth phase were seeded into 96-well plates (5,000 cells/well) and incubated for 24 h at 37˚C. Subsequently, 1, 3, 10, 30, 100 and 300 μmol/l of SFR were added to the 96-well plates. After following incubation for 12 h at 37˚C, 10 μl of CCK-8 reagent was added to the cells in each well and incubated for 2 h at 37˚C. The absorbance of each well was measured using a microplate reader at a wavelength of 450 nm. The viability of H9c2 cardiac myoblasts was calculated according to the manufacturer's protocol.

Evaluation of biochemical indexes. H9c2 cardiac myoblasts were prepared into $5x10^4$/ml cell suspension and inoculated in 96-well plates at 100 μl/well. Following treatment, LDH and CK-MB levels in cell supernatants were quantified using a microplate reader. The cell supernatants were collected and analyzed according to the manufacturer's protocol. Cells from each group were also digested with 0.25% trypsin, washed with PBS twice and ultrasonically pulverized to obtain a cell homogenate. This was then used to detect intracellular levels of GSH-Px, CAT, SOD, MDA and caspase-3 according to the corresponding manufacturer's protocol.

Detection of ROS levels. The common dichlorofluorescein, 2,7-dichlorodihydrofluorescein diacetate (DCFH-DA; cat. no. 85155: Cayman Chemical Company) was used to detect the levels of intracellular ROS in the present study. DCFH-DA can cross the cell membrane and enter the cell where it is hydrolyzed into DCFH by esterases. DCFH cannot cross the cell membrane, but non fluorescent DCFH can be oxidized by intracellular ROS to fluorescent DCF and, therefore, the intracellular ROS level can be quantified via fluorescence intensity (34). Following treatment, DCFH-DA (10 μmol/l) dye was added to each group and incubated for 20 min in the dark at 37˚C. Cells were imaged using a fluorescence microscope (magnification, x200; Nikon Eclipse C1; Nikon Corp). Image-Pro Plus 6.0 software (Media Cybernetics, Inc.) was used for quantification.

Analysis of ($[Ca^{2+}]_i$) concentration. H9c2 cardiac myoblasts were prepared into a $5x10^4$/ml cell suspension and inoculated in 96-well plates at 100 μl/well. Following treatment, the medium was replaced with PBS and H9c2 cardiac myoblasts were frozen at -20˚C, thawed and disrupted with an ultrasonic cell disruptor. H9c2 cardiac myoblasts were then centrifuged at 10,195 x g for 10 min at 4˚C and the supernatant was collected. The ($[Ca^{2+}]_i$) concentration in the supernatant was detected at a wavelength of 610 nm using a colorimetric method as stated in the Ca^{2+} assay kit, according to the manufacturer's protocol.

Detection of apoptosis and mitochondrial membrane potential (MMP). For quantification of apoptosis, flow cytometry was performed (FC500; Beckman Coulter, Inc.) using an Apoptosis Detection kit (cat. no. CA1050; Beijing Solarbio Science & Technology Co., Ltd.). Briefly, cells were suspended in 1X binding buffer at a cell density of $1x10^6$ cells/ml. To a centrifuge tube 100 μl of the cell suspension was added, followed by 5 μl of Annexin V-FITC and 5 μl PI. After mixing cells were incubated at 10˚C for 25 min before 500 μl PBS was added and cells were detected via flow cytometry (this step was carried out within 1 h). FlowJo 10 software (v10.6.2; BD Biosciences) was used to analyze the obtained flow cytometry data.

To detect the effects of SFR on MMP, the JC-1 MMP Detection kit (cat. no. M8650; Beijing Solarbio Science & Technology Co., Ltd.) was used. Following treatment, H9c2 cardiac myoblasts were incubated with JC-1 reagent (10 μg/ml) in the dark at 37˚C for 20 min, washed with PBS twice and detected via flow cytometry. FlowJo 10 software was used to analyze the obtained flow cytometry data.

Western blotting. The protein expression levels of PI3K, phosphorylated (p)-PI3K, AKT, p-AKT, GSK3β, p-GSK3β, B-cell lymphoma-2 (Bcl-2), Bcl-2 associated X protein (Bax), caspase-3 and cleaved caspase-3 were detected via western blotting. Following treatment, the H9c2 cardiac myoblasts were rinsed with precooled PBS buffer and RIPA buffer (cat. no. G2002; Wuhan Servicebio Technology, Co., Ltd.) was used to extract total protein. Total protein concentration was determined using the BCA protein assay kit and 30 μg protein/lane was separated by SDS-PAGE on a 10% gel. The separated proteins were transferred onto a PVDF membrane and subsequently blocked with 5% skimmed milk for 30 min at 37˚C. Membranes were subsequently incubated with the following primary antibodies against: Caspase-3 (1:1,000; cat. no. GB11767C), cleaved caspase-3 (1:1,000; cat. no. GB11532) (both from Wuhan Servicebio Technology Co., Ltd.), Bax (1:1,000; cat. no. 50599-2-Ig; ProteinTech Group, Inc.), Bcl-2 (1:500; cat. no. BM4985; Wuhan Boster Biological Technology, Ltd.), p-PI3K (1:600; cat. no. AF4372; Affinity Biosciences), PI3K (1:1,000; cat. no. ab151549; Abcam), p-GSK3β (1:1000; cat. no. AF2016; Affinity Biosciences), GSK3β (1:1,000; cat. no. AF7814; Affinity Biosciences), p-AKT (1:1,000; cat. no. 9611S; Cell Signaling Technology, Inc.), AKT (1:600; cat. no. 60203-2-Ig; ProteinTech Group, Inc.) and β-actin (1:1,000; cat. no. GB12001; Wuhan Servicebio Technology Co., Ltd.), overnight at 4˚C. After washing with PBS containing 0.05% Tween-20, the membranes were incubated with horseradish peroxidase-labelled secondary antibodies Goat anti-rabbit; (1:3,000; cat. no. ZB2301; Origene Technologies, Inc.) and Goat anti-mouse (1:3,000; cat. no. ZB2305; Origene Technologies, Inc.) at room temperature for 90 min. The gray values were semi-quantified using Tanon GIS software (version, Tanon GIS 2010; Tanon Science and Technology Co., Ltd.) after the film was imaged. β-actin was used as the internal reference gene.

Statistical analysis. Data analysis was performed using Origin version 9.1 software (OriginLab) and data are presented as the mean ± standard error of the mean (SEM). The statistical differences among three or more groups were analyzed using one-way analysis of variance (ANOVA) followed by Tukey's post hoc test. $P<0.05$ was considered to indicate a statistically significant difference.

Results

Effect of SFR on cell viability in H/R-induced H9c2 cardiac myoblasts. As demonstrated in Fig. 2A and B, cytotoxicity experiments in H9c2 cardiac myoblasts determined that $CoCl_2$ significantly inhibited cell viability in a dose-dependent manner compared with the CONT group. However, SFR treatment had no significant effect on the H9c2 cardiac myoblast viability. Therefore, 800 μmol/l $CoCl_2$ was chosen to induce hypoxia and 10 and 30 μmol/l SFR were used as low and high doses, respectively, to pre-protect H9c2 cardiac myoblasts. Fig. 2C demonstrates that maximum amount of H9c2 cell damage was significantly generated after 4 h of reoxygenation ($P<0.05$). Fig. 2D indicates that cell viability was significantly reduced in the H/R group compared with the CONT group ($P<0.01$). However, SFR treatment significantly increased the cell viability of H9c2 cardiac myoblasts in a dose-dependent manner compared with the H/R group ($P<0.01$). Furthermore, LY294002 significantly inhibited the protective effects of SFR on H/R-induced cardiomyoblast damage compared with the SFR_H + H/R group ($P<0.01$). The effects of SFR_A on H9c2 cardiac myoblasts were not significantly different compared with the CONT group. These results demonstrated that SFR could increase the viability of H9c2 cardiac myoblasts damaged by H/R, which may be related to the activation of PI3K/AKT/GSK3β signaling pathway.

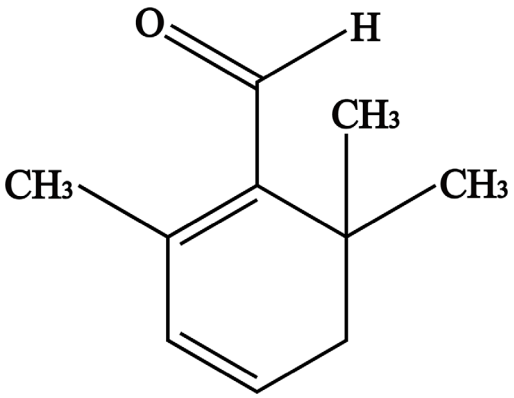

Figure 1. The chemical structure of safranal.

Effects of SFR on LDH and CK-MB levels. As displayed in Fig. 3, LDH and CK-MB levels were detected to assess H/R-induced H9c2 cardiac myoblast injury. Compared with the CONT group, CK-MB and LDH levels in the H/R group were significantly increased ($P<0.01$). However, SFR treatment significantly decreased the CK-MB and LDH levels compared with the H/R group ($P<0.05$ or $P<0.01$). Furthermore, LY294002 significantly inhibited the protective effect of SFR on H/R-induced cardiomyoblast damage compared with the SFR_H + H/R group ($P<0.01$). The effects of SFR_A on H9c2 cardiac myoblasts were not significantly different compared with the CONT group. These results indicated that SFR alleviated H/R-induced H9c2 cardiac myoblast injury, which may be associated with the activation of the PI3K/AKT/GSK3β signaling pathway.

Effect of SFR on oxidative stress. As displayed in Fig. 4, compared with the CONT group, SOD, CAT and GSH-Px levels were significantly decreased in the H/R group ($P<0.01$), whereas MDA levels were significantly increased ($P<0.01$). However, SFR treatment reversed these effects. SOD, CAT and GSH-Px levels were significantly increased, whereas MDA levels were significantly decreased in the SFR treated groups compared with the H/R group ($P<0.05$ or $P<0.01$). Furthermore, LY294002 significantly inhibited

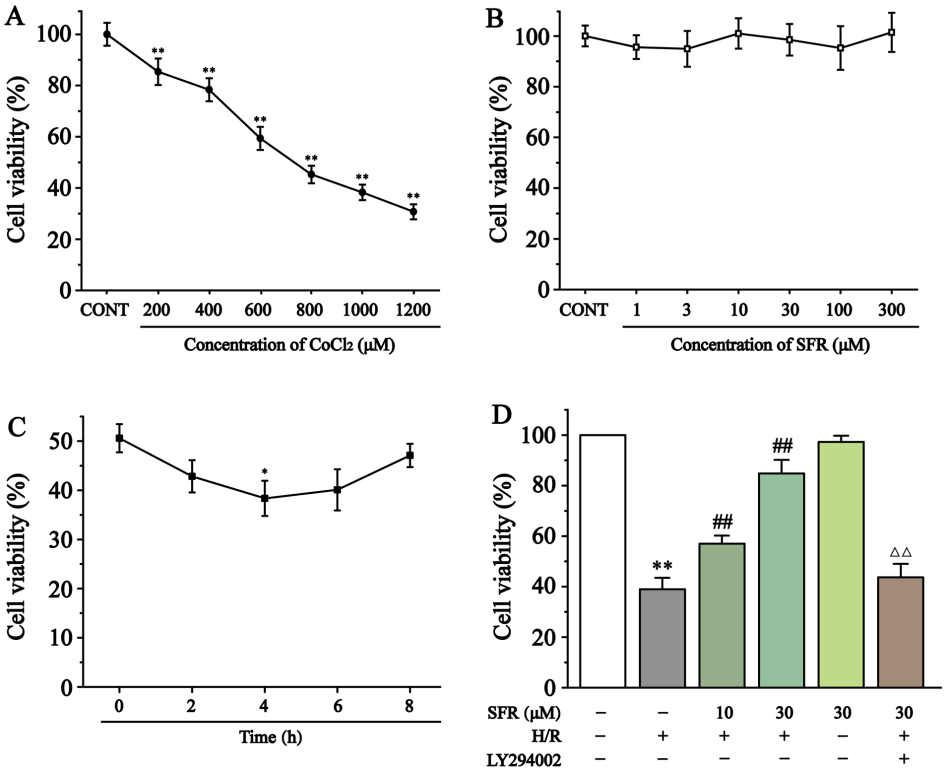

Figure 2. Effect of CoCl2 and SFR on the vitality of H9c2 cardiac myoblasts was detected using a CCK-8 assay. (A) H9c2 cardiac myoblasts were cultured with different concentrations of $CoCl_2$ for 24 h. **P<0.01 vs. CONT. (B) H9c2 cardiac myoblasts were cultured with different concentrations of SFR for 12 h. (C) Effect of reoxygenation time on the vitality of H9c2 cardiac myoblasts. *P<0.05 vs. Reoxygenation 0 h group. (D) The vitality of H9c2 cardiac myoblasts in CONT, H/R, SFR_L, SFR_H, SFR_A and LY294002 + SFR_H + H/R groups was detected using a CCK-8 assay. Data are presented as the mean ± SEM. n=6. **P<0.01 vs. CONT; $^{\#\#}$P<0.01 vs. H/R; and $^{\Delta\Delta}$P<0.01 vs. SFR_L, low dose SFR; SFR_H, high dose SFR; SFR_A, SFR alone. SFR_H + H/R. SFR, safranal; H/R, hypoxia/reoxygenation; CONT, control; CCK-8, Cell Counting Kit-8.

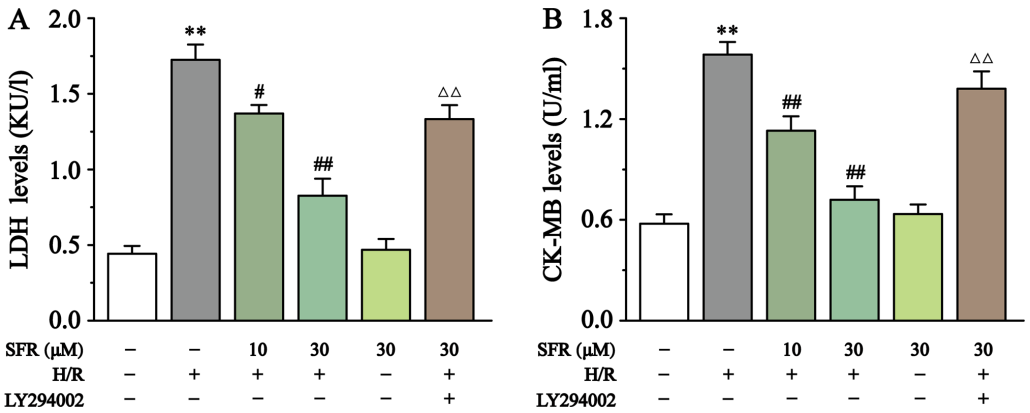

Figure 3. Effect of SFR on LDH and CK-MB levels. Effects of SFR treatment on (A) LDH and (B) CK-MB levels in H/R-induced H9c2 cardiac myoblasts. Data are presented as the mean ± SEM. n=6. **P<0.01 vs. CONT; $^{\#}$P<0.05, $^{\#\#}$P<0.01 vs. H/R; and $^{\Delta\Delta}$P<0.01 vs. SFR_H + H/R. SFR, safranal; LDH, lactate dehydrogenase; CK-MB, creatine kinase-MB; CONT, control; H/R, hypoxia/reoxygenation; SFR_H, high dose SFR.

the protective effect of SFR against H/R-induced oxidative stress damage (P<0.01) compared with the SFR_H + H/R group. The effects of SFR_A on H9c2 cardiac myoblasts were not significantly different compared with the CONT groups. These results indicated that SFR protected against H/R-induced oxidative stress injury, and this protective effect may be associated with the activation of the PI3K/AKT/GSK3β signaling pathway.

Effect of SFR on ROS levels. As displayed in Fig. 5, the ROS levels were detected by DCFH-DA. DCFH-DA is commonly used to detect ROS levels and when the intracellular ROS level increases a strong green fluorescence is exhibited. Compared with the CONT group, the H9c2 cardiac myoblasts in the H/R group exhibited significantly increased fluorescence and therefore ROS levels (P<0.01). However, SFR treatment reversed this effect and significantly decreased the fluorescence intensity and ROS levels compared with the H/R group (P<0.01). Furthermore, LY294002 significantly inhibited the effect of SFR on the H/R-induced increase of ROS levels compared with the SFR_H + H/R group (P<0.01). The effects of SFR_A on H9c2 cardiac myoblasts were not

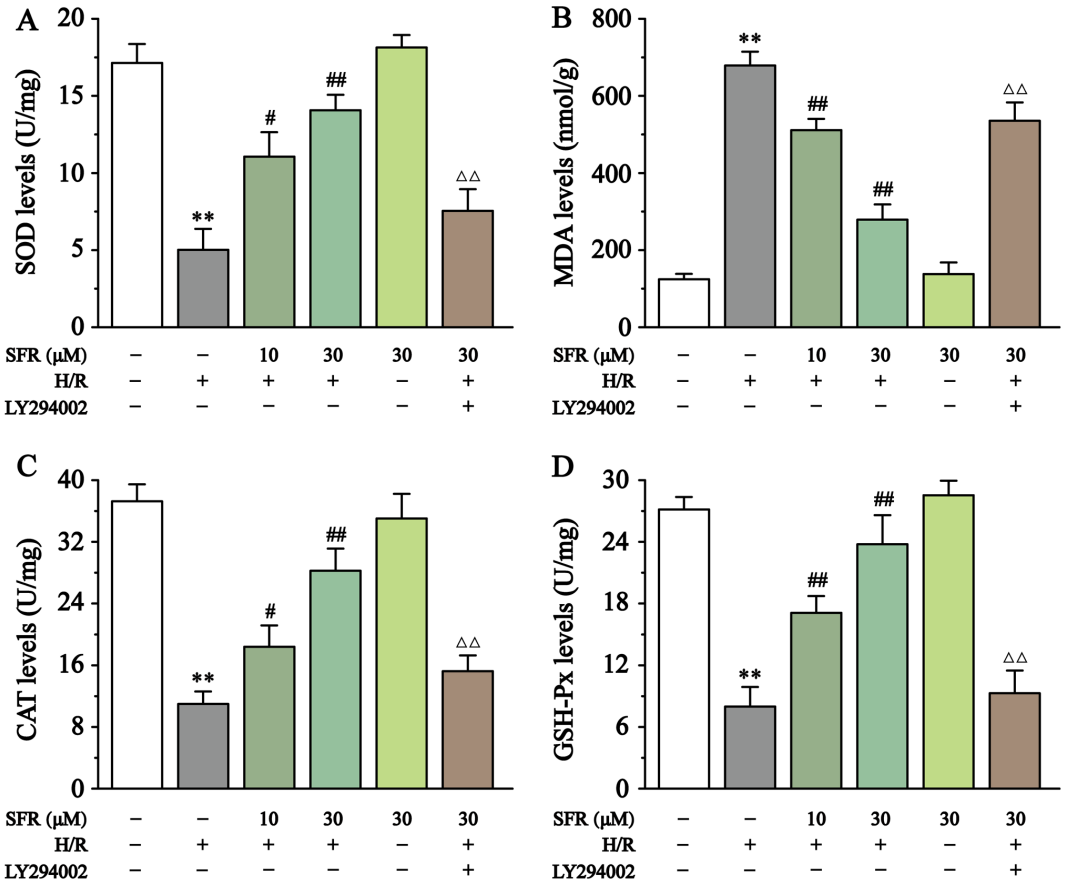

Figure 4. Effect of SFR on oxidative stress. Effect of SFR on (A) SOD, (B) MDA, (C) CAT and (D) GSH-Px. Data are presented as the mean ± SEM. n=6. **P<0.01 vs. CONT; $^{\#}$P<0.05, $^{\#\#}$P<0.01 vs. H/R; and $^{\Delta\Delta}$P<0.01 vs. SFR_H + H/R. SFR, safranal; SOD, superoxide dismutase; MDA, malondialdehyde; CAT, catalase; GSH-Px, glutathione peroxidase; CONT, control; H/R, hypoxia/reoxygenation; SFR_H, high dose SFR.

significantly different compared with the CONT group. These results suggested that SFR could decrease the ROS levels induced by H/R, which may be related to the activation of PI3K/AKT/GSK3β signaling pathway.

Effect of SFR on MMP levels. As displayed in Fig. 6A and B, MMP levels in each group were quantified using flow cytometry. The change of MMP is an important parameter that reflects mitochondrial viability and can be detected by JC-1, a lipophilic fluorescent dye (35). At high levels of MMP, JC-1 converges to form polymers in the mitochondrial matrix and produces red fluorescence. At low levels of MMP, JC-1 cannot aggregate in the mitochondrial matrix and only produces green fluorescence as a monomer. The subsequent change in levels of MMP are detected by the relative proportion of red:green fluorescence. The levels of MMP were significantly decreased by H/R in H9c2 cardiac myoblasts compared with the CONT group (P<0.01). However, SFR treatment significantly increased the level of MMP compared with the H/R group (P<0.05 or P<0.01). Furthermore, LY294002 significantly inhibited the effect of SFR on the H/R-induced decrease of MMP compared with the SFR_H + H/R group (P<0.01). The effects of SFR_A on H9c2 cardiac myoblasts were not significantly different compared with the CONT group. These results indicated that SFR protected against H/R-induced reduction of MMP, and this protective effect may be associated with the activation of the PI3K/AKT/GSK3β signaling pathway.

Effect of SFR on ($[Ca^{2+}]_i$) concentration. As displayed in Fig. 6C, the effect of SFR on ($[Ca^{2+}]_i$) concentration was detected. The results demonstrated that ($[Ca^{2+}]_i$) concentration was significantly increased in the H/R group compared with the CONT group (P<0.01). However, compared with the H/R group, SFR treatment significantly decreased the ($[Ca^{2+}]_i$) concentration (P<0.01). Furthermore, LY294002 significantly inhibited the protective effects of SFR on H/R-induced ($[Ca^{2+}]_i$) overload compared with the SFR_H + H/R group (P<0.01). The effects of SFR_A on H9c2 cardiac myoblasts were not significantly different compared with the CONT group. These results suggested that SFR alleviated H/R-induced ($[Ca^{2+}]_i$) overload, which may be associated with the activation of the PI3K/AKT/GSK3β signaling pathway.

Effect of SFR on apoptotic rate. The effect of SFR on apoptotic rate was determined using flow cytometry as displayed in Fig. 7. The results demonstrated that the apoptotic rate in the H/R group was significantly upregulated compared with the CONT group (P<0.01), whereas SFR treatment significantly decreased the H/R-induced increase apoptotic rate compared with the H/R group (P<0.01).

Fig. 8 displays the effect of SFR on caspase-3, cleaved caspase-3, Bcl-2 and Bax protein expression levels in H/R-induced H9c2 cardiac myoblast injury. Compared with the CONT group, Bcl-2 protein expression levels were significantly decreased in the H/R group, whereas caspase-3, cleaved

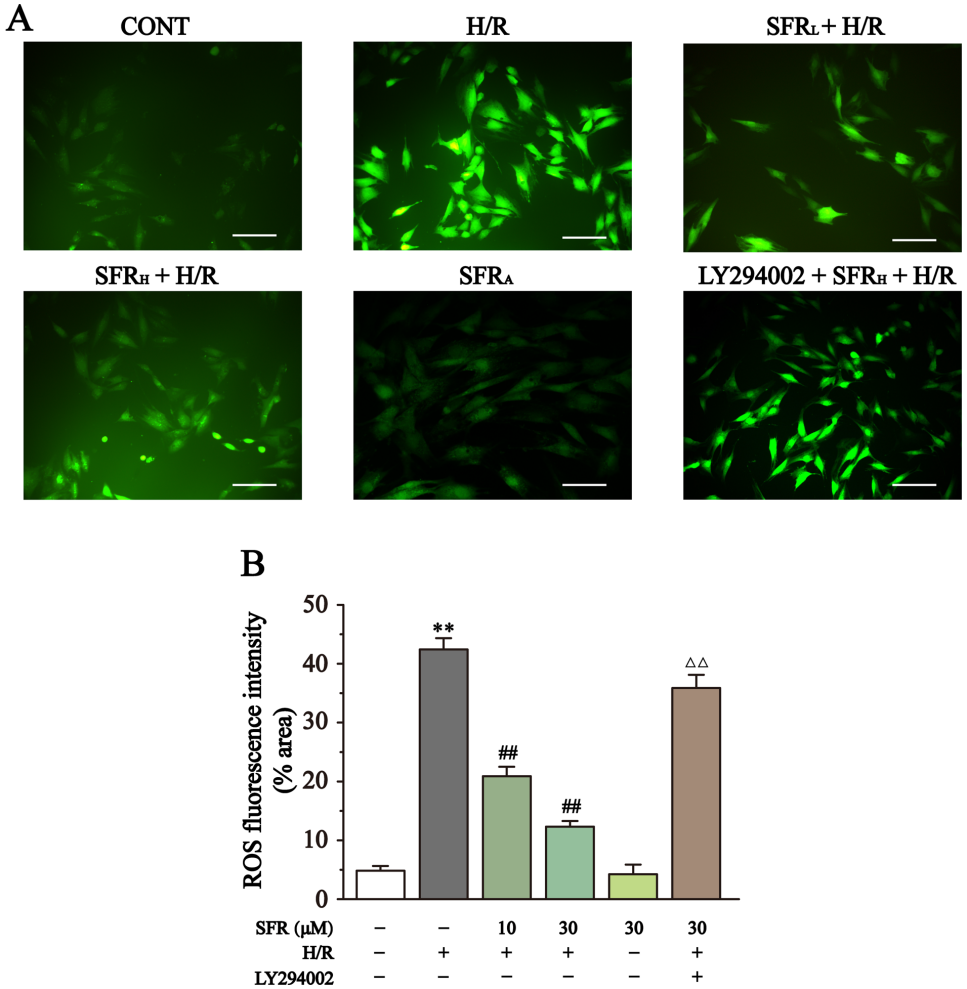

Figure 5. Effect of SFR on ROS levels. (A) Representative ROS fluorescence images (magnification, x200; scale bar, 100 μm) from CONT, H/R, SFR_L + H/R, SFR_H + H/R, SFR_A and LY294002 + SFR_H + H/R groups. (B) ROS fluorescence intensity. Data are presented as the mean ± SEM. n=6. **P<0.01 vs. CONT; $^{\#\#}$P<0.01 vs. H/R; $^{\Delta\Delta}$P<0.01 vs. SFR_H + H/R. SFR, safranal; H/R, hypoxia/reoxygenation; CONT, control; ROS, reactive oxygen species; SFR_L, low dose SFR; SFR_H, high dose SFR; SFR_A, SFR alone.

caspase-3 and Bax protein expression levels were significantly upregulated (P<0.01). However, SFR treatment reversed this effect. SFR treatment could significantly decrease caspase-3, cleaved caspase-3 and Bax protein expression levels and significantly increased the protein expression levels of Bcl-2 compared with the H/R group (P<0.05 or P<0.01). These results indicated that SFR alleviated H/R-induced apoptotic damage. Furthermore, as displayed in Fig. 8F and G, the results of caspase-3, cleaved caspase-3, Bax and Bcl-2 protein expression levels demonstrated that LY294002 significantly inhibited the protective effects of SFR on H/R-induced cardiomyocyte apoptosis compared with the SFR_H + H/R group (P<0.01). The effects of SFR_A on H9c2 cardiac myoblasts were not significantly different compared with the CONT group. These results indicated that SFR alleviated H/R-induced apoptotic damage, which may be associated with the activation of the PI3K/AKT/GSK3β signaling pathway.

Effect of SFR on the protein expression levels of AKT, p-AKT, PI3K, p-PI3K, GSK3β and p-GSK3β. Fig. 9 displays the effects of SFR on the PI3K/AKT/GSK3β signaling pathway in H/R-induced H9c2 cardiac myoblasts. The results demonstrated that p-AKT/AKT, p-PI3K/PI3K and p-GSK3β/GSK3β protein expression levels in the H/R group were significantly decreased compared with the CONT group (P<0.01). Compared with the H/R group, the protein expression levels of p-AKT/AKT, p-PI3K/PI3K and p-GSK3β/GSK3β were significantly increased when treated with SFR (P<0.05 or P<0.01). Furthermore, LY294002 significantly inhibited the effect of SFR on the protein expression levels of p-AKT/AKT, p-PI3K/PI3K and p-GSK3β/GSK3β in H9c2 cardiac myoblasts exposed to $CoCl_2$, compared with the SFR_H + H/R group (P<0.01). No significant difference was observed in the protein expression levels of p-AKT/AKT, p-PI3K/PI3K and p-GSK3β/GSK3β between the CONT group and the SFR_A group. These results suggested that SFR alleviated H9c2 cardiac myoblast injury induced by H/R via regulation of the PI3K/AKT/GSK3β pathway.

Effect of SFR post-treatment on the viability of H9c2 cardiac myoblasts and LDH, CK-MB, SOD, MDA and caspase-3 levels. Fig. S1 displays the protective effects of SFR post-treatment on H/R-induced H9c2 cardiac myoblast injury. The results demonstrated that compared with the control group, the H9c2 cardiac myoblast viability and SOD levels in the H/R group were significantly reduced, whereas LDH, CK-MB, MDA and caspase-3 levels were significantly

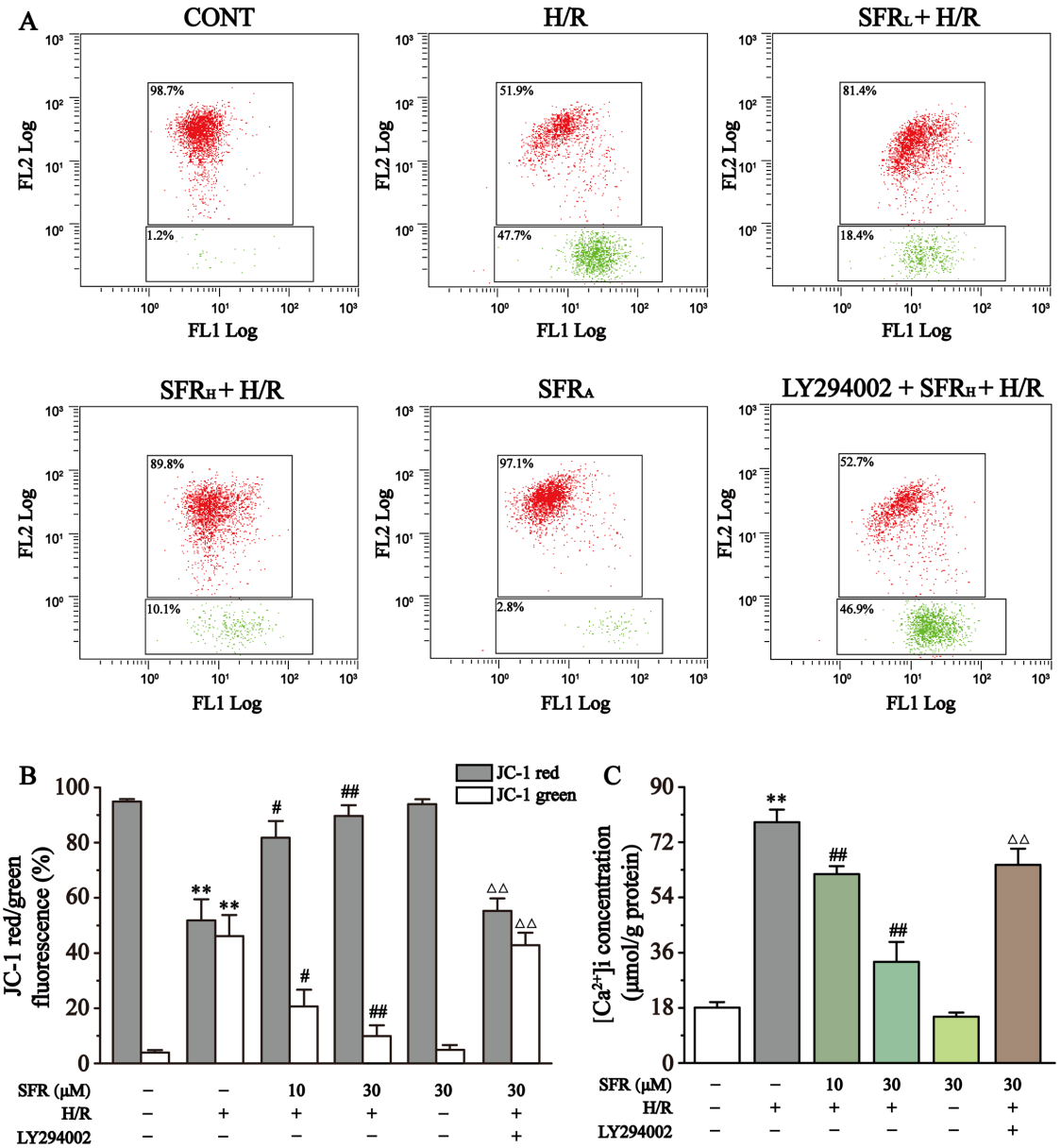

Figure 6. Effect of SFR on MMP and $[Ca^{2+}]_i$ concentration. (A) Flow cytometry analysis of the CONT, H/R, SFR_L + H/R, SFR_H + H/R, SFR_A and LY294002 + SFR_H + H/R groups. (B) Data summary of MMP flow cytometry results. n=3. (C) $[Ca^{2+}]_i$ concentration. n=6. Data are represented as the mean ± SEM. **P<0.01 vs. CONT; $^{\#}$P<0.05, $^{\#\#}$P<0.01 vs. H/R group; and $^{\Delta\Delta}$P<0.01 vs. SFR_H + H/R. SFR, safranal; H/R, hypoxia/reoxygenation; CONT, control; SFR_L, low dose SFR; SFR_H, high dose SFR; SFR_A, SFR alone; $[Ca^{2+}]_i$, intracellular Ca^{2+}.

increased (P<0.01). However, SFR post-treatment reversed this effect. Compared with the H/R group, SFR post-treatment significantly increased H9c2 cardiac myoblast viability and SOD levels, whereas LDH, CK-MB, MDA and caspase-3 levels were significantly decreased (P<0.05 or P<0.01). These results indicated that SFR post-treatment also has a certain protective effect against H/R-induced H9c2 cardiac myoblast injury. Furthermore, the effects of SFR only on H9c2 cardiac myoblasts were not significantly different compared with the control group. These results suggested that SFR alleviated H9c2 cardiac myoblast injury induced by H/R.

Discussion

CVDs are the main causes of mortality worldwide and are currently difficult to treat (36). CVD was the primary cause of 17.7 million deaths worldwide in 2015, which is predicted to increase to 23.6 million by 2030 (37,38). SFR, the main active substance extracted from saffron, has been proven to have cardio-protective properties (30-32). However, to the best of our knowledge, there are no published studies investigating the protective effect of SFR against H/R-induced myocardial injury *in vitro*.

Therefore, the present study investigated the effect of SFR on MIRI *in vitro*, which excluded disturbances caused by neural and humoral reflex regulation *in vivo*, more clearly demonstrating the therapeutic effect of SFR. The results demonstrated that SFR can protect against MIRI by acting directly on cardiomyoblasts. Moreover, previous studies have reported that $CoCl_2$ can inhibit H9c2 cell viability and induce apoptosis in a dose-dependent manner (39-41). Apoptotic death of cardiomyocytes is an important pathological feature

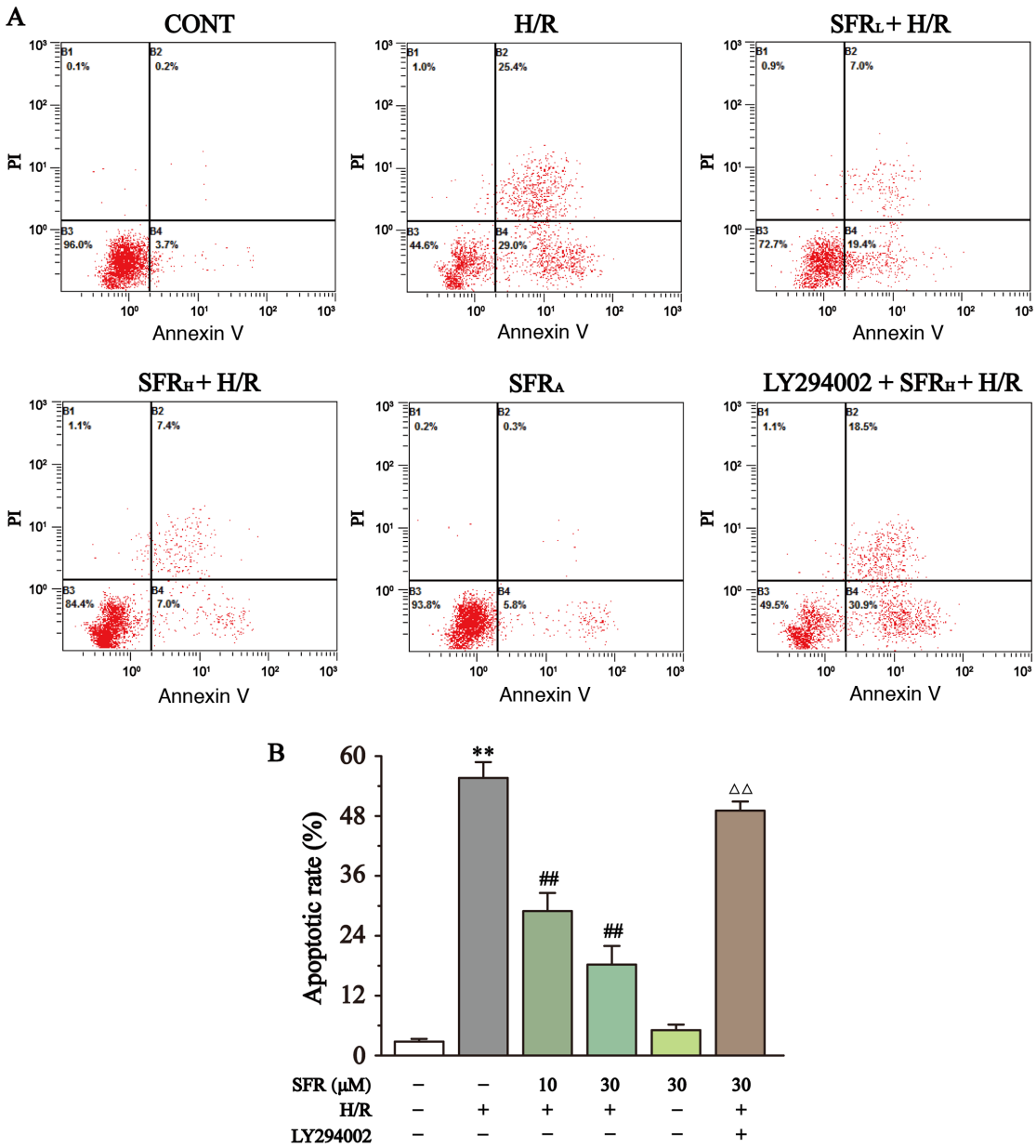

Figure 7. Effects of SFR on cell apoptosis. (A) Flow cytometry analysis of CONT, H/R, SFR_L + H/R, SFR_H + H/R, SFR_A and LY294002 + SFR_H + H/R groups. (B) Data summary of apoptotic rate flow cytometry analysis. Data are represented as the mean ± SEM. n=3. **P<0.01 vs. CONT; $^{\#\#}$P<0.01 vs. H/R; and $^{\Delta\Delta}$P<0.01 vs. SFR_H + H/R. SFR, safranal; H/R, hypoxia/reoxygenation; CONT, control; SFR_L, low dose SFR; SFR_H, high dose SFR; SFR_A, SFR alone.

observed in MIRI (9). Therefore, using $CoCl_2$ to establish a hypoxia model was beneficial for exploring the regulatory mechanism of SFR on hypoxia- induced apoptosis and for demonstrating the myocardial protective effect of SFR. The results of the present study demonstrated that both SFR pre-treatment and post-treatment significantly increased H9c2 cell viability in the H/R group. Furthermore, the protective effects of SFR on H/R-induced damage were demonstrated via quantification of oxidative stress, apoptosis, ($[Ca^{2+}]_i$) overload, MMP and the associated signaling pathway.

$CoCl_2$ is commonly used for chemical hypoxia simulation during *in vitro* experiments (42). Ca^{2+} in $CoCl_2$ can replace the Fe^{2+} in the hemoglobin porphyrin ring, so that hemoglobin cannot bind oxygen and remains in a reduced state, thereby imitating an hypoxic environment and producing a series of reactions similar to those in hypoxic conditions (43). Moreover, under normoxic conditions, $CoCl_2$ can strongly stabilize hypoxia-inducible factor (HIF)-1α and HIF-2α, which are heterodimeric transcription factors composed of an oxygen-regulated α subunit (42). Compared with low oxygen-induced hypoxia and the use of other hypoxia mimics, the stabilization of HIF-1α and HIF-2α is sustained for several hours (42). Therefore, this model in normoxic conditions provides more time in which samples can be analyzed (42). The cardiac myoblast H9c2 cell line is an immortalized cell line isolated from rat embryonic heart tissue (44). H9c2 cells show morphological characteristics similar to those of immature embryonic cardiocytes but have preserved several elements of the electrical and hormonal signal pathway found in adult cardiac cells (44). H9c2 cardiac myoblasts have been commonly used for experimental studies of cardiomyocyte physiology and pathology because of their similar physiological

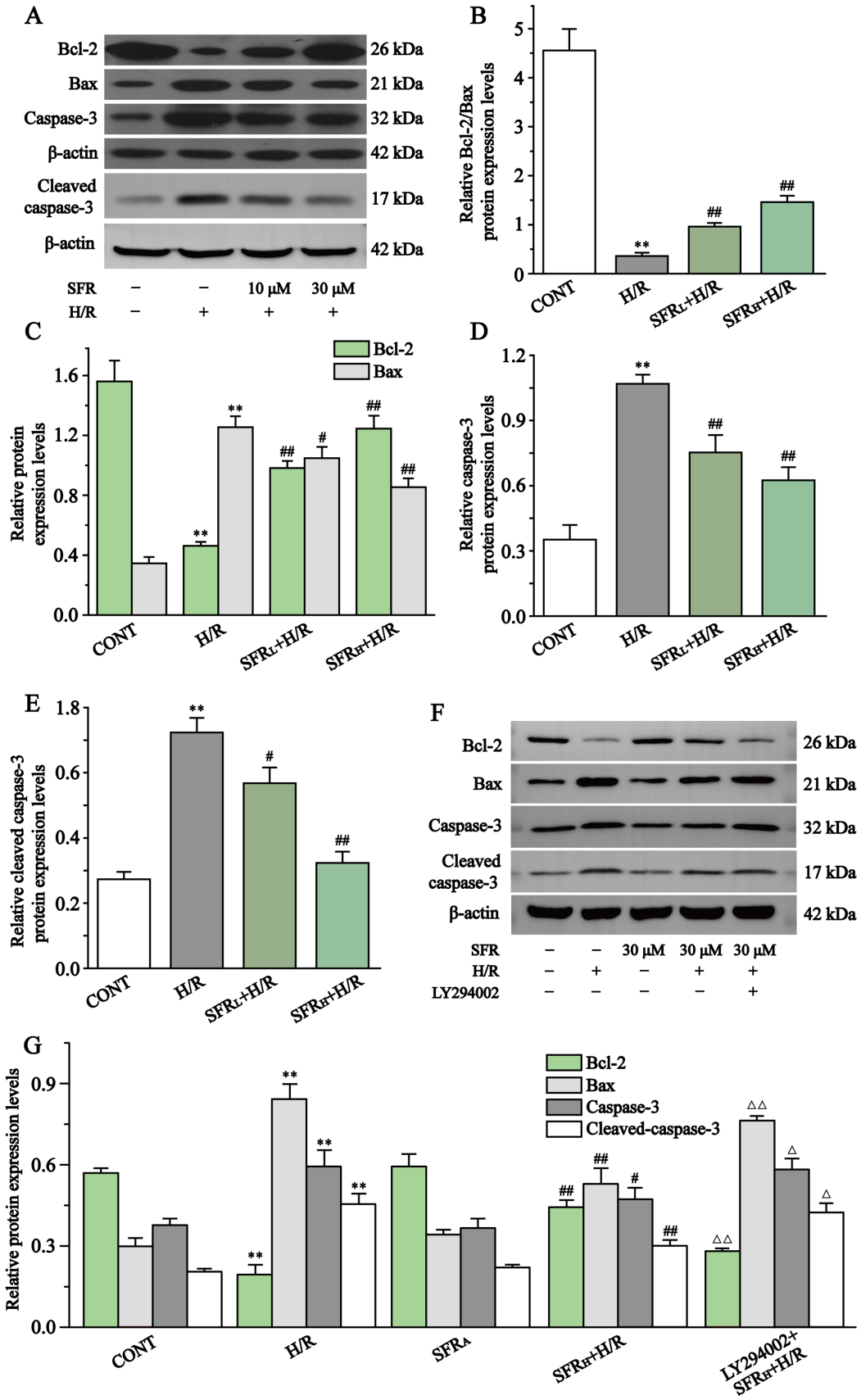

Figure 8. Effect of SFR on the protein expression levels of Bax, Bcl-2, caspase-3 and cleaved caspase-3. (A) Western blot analysis of the Bcl-2, Bax, capase-3 and cleaved caspase-3 expression levels in CONT, H/R, SFR_L + H/R and SFR_H + H/R groups. (B) The ratio of Bcl-2 to Bax expression levels normalized to β-actin. (C) Quantification of the Bcl-2 and Bax protein expression levels normalized to β-actin. Quantification of the (D) capase-3 and (E) cleaved caspase-3 protein expression levels normalized to β-actin. (F) Western blot analysis of Bax, Bcl-2, capase-3 and cleaved caspase-3 in CONT, H/R, SFR_L + H/R, SFR_H + H/R, SFR_A and LY294002 + SFR_H + H/R groups. (G) Quantification of the Bcl-2, Bax, capase-3 and cleaved caspase-3 protein expression levels normalized to β-actin. Data are presented as the mean ± SEM. n=3 **P<0.01 vs. CONT; $^{\#}$P<0.05, $^{\#\#}$P<0.01 vs. H/R; and $^{\Delta}$P<0.05, $^{\Delta\Delta}$P<0.01 vs. SFR_H + H/R. SFR_L, low dose SFR; SFR_H, high dose SFR; SFR_A, SFR alone. SFR, safranal; H/R, hypoxia/reoxygenation; CONT, control.

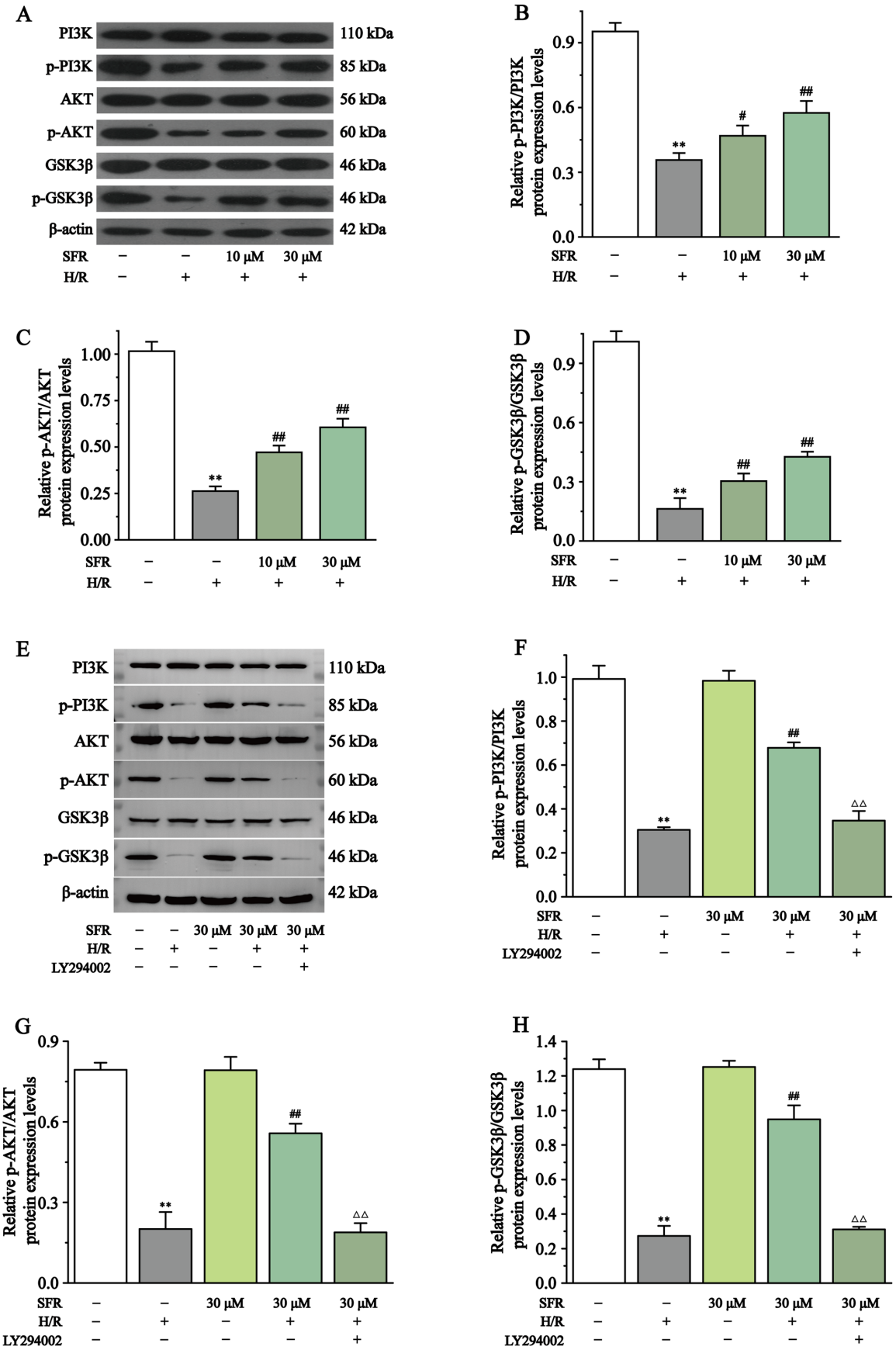

Figure 9. Effect of SFR on the PI3K/AKT/GSK3β signaling pathway protein expression levels. (A) Western blot analysis of the PI3K, p-PI3K, AKT, p-AKT, GSK3β and p-GSK3β expression levels in CONT, H/R, SFR_L + H/R and SFR_H + H/R groups. The ratio of (B) p-PI3K to PI3K, (C) p-AKT to AKT and (D) p-GSK3β to GSK3β normalized to β-actin. (E) Western blot analysis of the PI3K, p-PI3K, AKT, p-AKT, GSK3β and p-GSK3β expression levels in CONT, H/R, SFR_H + H/R, SFR_A and LY294002 + SFR_H + H/R groups. The ratio of (F) p-PI3K to PI3K, (G) p-AKT to AKT and (H) p-GSK3β to GSK3β normalized to β-actin. Data are presented as the mean ± SEM. n=3. **P<0.01 vs. CONT; $^{\#}$P<0.05, $^{\#\#}$ P<0.01 vs. H/R; and $^{\Delta\Delta}$P<0.01 vs. SFR_H + H/R. SFR_L, low dose SFR; SFR_H, high dose SFR; SFR_A, SFR alone. SFR, safranal; CONT, control; H/R, hypoxia/reoxygenation; p, phosphorylated.

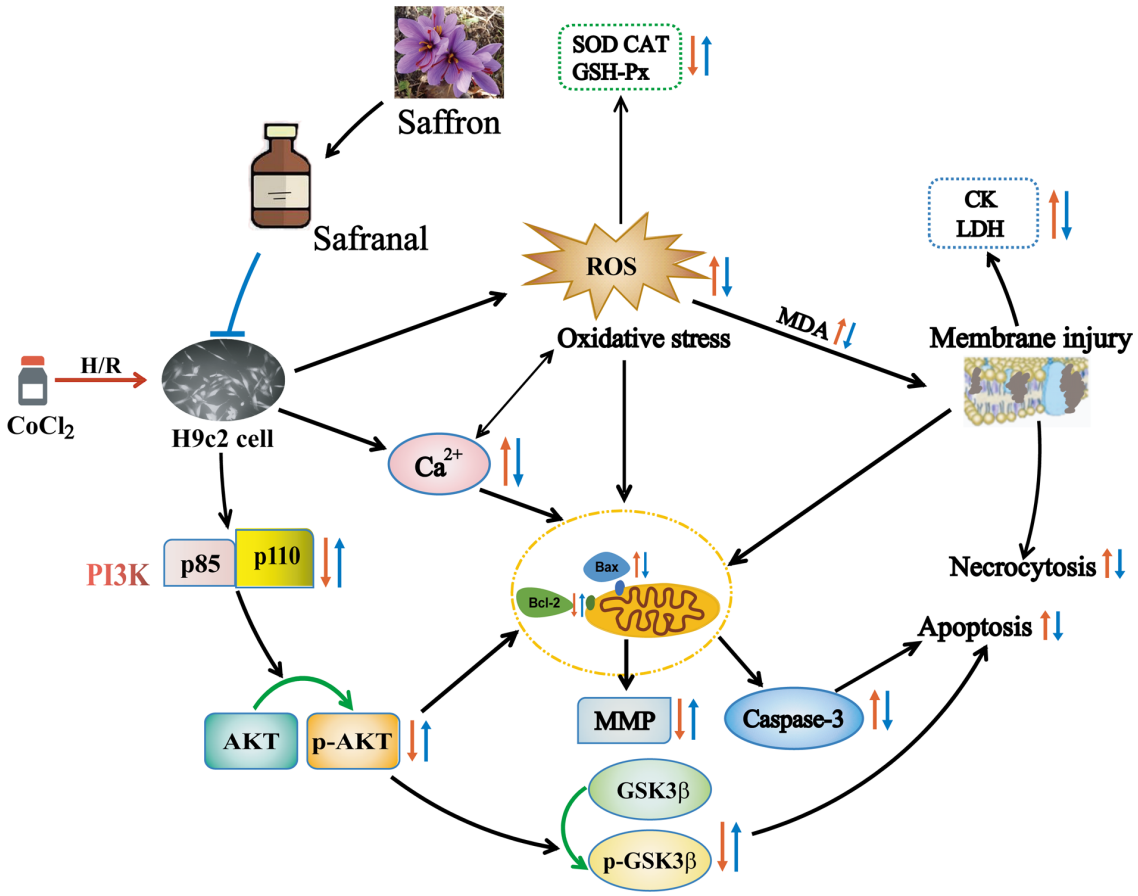

Figure 10. Mechanism for the protective effects of safranal. Red arrow, damage caused by H/R. The direction of the red arrow represents the trend of oxidative stress- and apoptosis-related indicators, and PI3K/AKT/GSK3β pathway protein expression caused by H/R. Blue arrow, protective effect of SFR. The direction of the blue arrow represents the effect of SFR on indicators associated with oxidative stress and apoptosis, and PI3K/AKT/GSK3β pathway protein expression. ROS, reactive oxygen species; H/R, hypoxia/reoxygenation; SOD, superoxide dismutase; MDA, malondialdehyde; CAT, catalase; GSH-Px, glutathione peroxidase; LDH, lactate dehydrogenase; CK-MB, creatine kinase-MB.

characteristics to adult rat cardiomyocytes in terms of electrophysiology and signal transduction (44). The predictors of cardiac pathological changes are CK-MB and LDH, which are stable cytosolic enzymes in cardiomyocytes (45-47). When the myocardial cell membrane is damaged, CK-MB and LDH are rapidly released from the cells into the culture medium (47). In the present study, the results demonstrated that both SFR pre-treatment and post-treatment significantly reduced the LDH and CK-MB levels, indicating that SFR may attenuate H/R-induced cardiomyoblast injury.

MIRI is a process that causes oxidative stress, whereby a large number of ROS are generated via multiple pathways, endogenous free radical scavenging systems dysfunction and ROS aggregation occurs within the body (48). ROS accumulation results in cardiomyocyte dysfunction, which further causes intracellular protein denaturation and degradation, loss of cellular function and results in the cytochrome oxidase system delivering significantly fewer electrons, leading to energy metabolism disorders (49). MIRI is often accompanied by intense lipid peroxidation that dysregulates the unsaturated fatty acid/protein ratio of the cell membrane. This results in enhanced cell membrane permeability and destruction of the antioxidant enzyme activity within the cell (48). MDA is an oxidative end product of oxygen radicals acting on lipids; thus, levels of MDA reflect the extent of oxygen free radical damage to cells (50). The antioxidant enzyme activities of GSH-Px, CAT and SOD can reflect the body's ability to scavenge oxygen free radicals (51).

A previous study has reported that spices containing phenolic and flavonoid compounds have antioxidant properties (52). The antioxidant capacities of saffron are mainly attributed to its active constituents, including SFR, crocin and crocetin, which have been determined to have antioxidant effects (53). The antioxidant effects of SFR may be associated with the aldehyde group in its structure, which has strong reducing properties. Furthermore, in a previous study on the oxygen radical scavenging ability of SFR, Assimopoulou *et al* (54) attributed the antioxidant effect of SFR to its ability to donate hydrogen atoms to 2,2-diphenyl-1-picrylhydrazyl radicals (54). In the present study, the results demonstrated that SFR significantly reduced ROS and MDA levels but significantly enhanced SOD, CAT and GSH-Px levels. These results indicated that SFR may exert cardiomyoblast protective effects by enhancing the body's scavenging ability against oxygen free radicals and alleviating lipid peroxidation injury in the cell membrane. However, the inhibitor LY294002 reversed the aforementioned beneficial effects of SFR, demonstrating that the protective effects of SFR against H/R-induced injury are associated with the activation of the PI3K/AKT/GSK3β signaling pathway. Furthermore, SFR post-treatment significantly increased

SOD levels but decreased MDA levels, indicating that SFR post-treatment may also have a protective effect against H/R-induced oxidative stress injury.

Mitochondria, the major site of cellular oxidative phosphorylation, serve an important role in the process of cell necrosis and apoptosis induced by MIRI. In normal physiological conditions, the mitochondrial permeability transition pore (mPTP) is in the closed state. When MIRI occurs, factors such as ($[Ca^{2+}]_i$) overload and oxidative stress can stimulate mPTP opening (55,56). As a result, the homeostasis of ($[Ca^{2+}]_i$) is destroyed, leading to increased Ca^{2+} influx, unbalanced free Ca^{2+} reuptake and Ca^{2+} accumulation in the cytoplasm (57). The opening of mPTP can further lead to mitochondrial swelling, mitochondrial destruction, cytochrome c release from mitochondria into the cytosol and activation of the caspase family, which induces apoptosis (58).

Apoptosis is one of the major forms of cell death during MIRI (59), which is a pathological process that is controlled by a variety of genes and mediated via signaling pathways, such as PI3K/AKT (60), Wnt (61) and JNK (62) signaling pathways. Apoptosis is therefore controlled by complex regulatory mechanisms (60). Both Bax and Bcl-2 belong to the Bcl-2 family, in which Bcl-2 is an apoptosis suppressor gene and Bax is a proapoptotic gene, with the two interacting together to regulate apoptosis (63). Jayanthi *et al* (64) reported that the regulation of apoptosis is dependent on the Bcl-2/Bax ratio, and that the lower the Bcl-2/Bax ratio, the higher the degree of apoptosis. The caspase protein family are important cell regulatory genes, which are involved in the initiation and regulation of apoptosis. Caspase-3 is considered to be a key protease activated by various apoptotic stimuli (65). In the present study, the results demonstrated that SFR significantly elevated MMP levels, while it decreased ($[Ca^{2+}]_i$) concentration and the apoptotic rate of H/R-induced H9c2 cardiac myoblasts, improving cell survival. Furthermore, western blotting demonstrated that SFR significantly inhibited the caspase-3, cleaved caspase-3 and Bax protein expression levels and significantly upregulated Bcl-2 protein expression levels. However, LY294002 reversed the aforementioned beneficial effects of SFR and therefore demonstrated that the protective effects of SFR against H/R-induced injury may be associated with the activation of the PI3K/AKT/GSK3β signaling pathway. Furthermore, SFR post-treatment significantly decreased caspase-3 levels, suggesting that SFR post-treatment also has a protective effect against H/R-induced apoptosis.

The intracellular PI3K/AKT/GSK3β signal transduction pathway serves important biological roles in cellular mechanisms, such as apoptosis, cell survival and proliferation (66). During MIRI, the RISK signaling pathway is activated and the expression levels of numerous types of proteins with endogenous protective effects increase (14). PI3K, which serves a key role in the RISK signaling pathway, is activated, causing downstream AKT to transfer from the cytosol to the cell membrane (67). AKT translocates from the cytosol to the cell membrane and undergoes a conformational change, which is subsequently activated by phosphorylation at the Ser473 site. Activated AKT exhibits anti-myocardial ischemia/hypoxia and anti-myocardial apoptosis effects (68). p-AKT further promotes the phosphorylation of downstream GSK3β proteins, thereby reducing the activation of caspase-3 and closing the mPTP to exert cell survival, antioxidant and antiapoptotic effects (69,70). p-AKT can also activate Bcl-2, reducing the activation of Bax and stabilizing the inner and outer mitochondrial membranes to further exert antiapoptotic effects (71). The results of the present study demonstrated that SFR significantly increased the phosphorylation levels of PI3K, AKT and GSK3β. However, the protein expression levels of apoptosis-related proteins were significantly decreased when cells were treated with SFR. These results demonstrated that the activation of caspase-3 may be inhibited by SFR, which may be associated with the activation of the PI3K/AKT/GSK3β signaling pathway. In order to further confirm that the myocardial protective effect of SFR was associated with the activation of the PI3K/AKT/GSK3β signaling pathway, the PI3K/AKT specific inhibitor LY294002 was used for further verification. The results demonstrated that LY294002 significantly inhibited the effects of SFR on PI3K/AKT/GSK3β signaling pathway apoptosis-related protein expression levels, demonstrating the important role of the PI3K/AKT/GSK3β signaling pathway in combating H/R injury.

In conclusion, SFR has been demonstrated to alleviate H/R-induced cardiomyocyte injury and reduce oxidative stress, ($[Ca^{2+}]_i$) overload and apoptotic rate, which are associated with the involvement of SFR in the regulation of the PI3K/AKT/GSK3β signaling pathway. The present study provides a theoretical basis for investigating the use of SFR as a therapeutic for the treatment of MIRI. However, the present study has certain limitations. We used H9c2 cardiac myoblasts to study the protective effect of SFR *in vitro*, although with the advantages of easy operation and the ability to intuitively reflect the effects of the studied drugs, compared with *in vivo* experiments, certain processes cannot be simulated *in vitro*. Therefore, further exploration is still needed.

Acknowledgements

Not applicable.

Funding

The present study was supported by the Research Fund of Administration of Traditional Chinese Medicine of Hebei Province (grant no. 2019081) and the Research Foundation of Hebei University of Chinese Medicine (grant nos. YTZ2019003 and KTZ2019009).

Availability of data and materials

The datasets used and/or analyzed during the current study are available from the corresponding author on reasonable request.

Authors' contributions

JS, YL and SS designed and planned the study. HeW, BZ, KC and XH carried out the experiments. BZ, HoW and LL performed the data analysis. HeW wrote the original draft. BZ, KC, XH, LL, JS and YL reviewed and edited the manuscript. JS and YL supervised the project. SS was involved in the identification of resources. HeW and SS confirm the authenticity of all the raw data. All authors have read and approved the final manuscript.

Ethics approval and consent to participate

Not applicable.

Patient consent for publication

Not applicable.

Competing interests

The authors declare that they have no competing interests.

References

1. Sanderson JE, Mayosi B, Yusuf S, Reddy S, Hu S, Chen Z and Timmis A: Global burden of cardiovascular disease. Heart 93: 1175, 2007.
2. Mahmood SS, Levy D, Vasan RS and Wang TJ: The Framingham Heart Study and the epidemiology of cardiovascular disease: A historical perspective. Lancet 383: 999-1008, 2014.
3. Zhang G, Gao S, Li X, Zhang L, Tan H, Xu L, Chen Y, Geng Y, Lin Y, Aertker B, *et al*: Pharmacological postconditioning with lactic acid and hydrogen rich saline alleviates myocardial reperfusion injury in rats. Sci Rep 5: 9858, 2015.
4. Najib K, Boateng S, Sangodkar S, Mahmood S, Whitney H, Wang CE, Racsa P and Sanborn TA: Incidence and characteristics of patients presenting with acute myocardial infarction and non-obstructive coronary artery disease. Catheter Cardiovasc Interv 86 (Suppl 1): S23-S27, 2015.
5. O'Neill WW, Topol EJ and Pitt B: Reperfusion therapy of acute myocardial infarction. Prog Cardiovasc Dis 30: 235-266, 1988.
6. Braunwald E and Kloner RA: Myocardial reperfusion: A double-edged sword? J Clin Invest 76: 1713-1719, 1985.
7. Hausenloy DJ and Yellon DM: Targeting myocardial reperfusion injury-the search continues. N Engl J Med 373: 1073-1075, 2015.
8. Jennings RB: Historical perspective on the pathology of myocardial ischemia/reperfusion injury. Circ Res 113: 428-438, 2013.
9. Turer AT and Hill JA: Pathogenesis of myocardial ischemia-reperfusion injury and rationale for therapy. Am J Cardiol 106: 360-368, 2010.
10. Moens AL, Claeys MJ, Timmermans JP and Vrints CJ: Myocardial ischemia/reperfusion-injury, a clinical view on a complex pathophysiological process. Int J Cardiol 100: 179-190, 2005.
11. Cheng BC, Huang HS, Chao CM, Hsu CC, Chen CY and Chang CP: Hypothermia may attenuate ischemia/reperfusion-induced cardiomyocyte death by reducing autophagy. Int J Cardiol 168: 2064-2069, 2013.
12. Reeve JL, Duffy AM, O'Brien T and Samali A: Don't lose heart - therapeutic value of apoptosis prevention in the treatment of cardiovascular disease. J Cell Mol Med 9: 609-622, 2005.
13. Blebea J, Kerr JC, Padberg FT Jr and Hobson RW II: Triphenyl tetrazolium chloride as a histochemical marker of skeletal muscle ischemia and reperfusion injury. Curr Surg 44: 134-136, 1987.
14. Heusch G: Molecular basis of cardioprotection: Signal transduction in ischemic pre-, post-, and remote conditioning. Circ Res 116: 674-699, 2015.
15. Hausenloy DJ and Yellon DM: Survival kinases in ischemic preconditioning and postconditioning. Cardiovasc Res 70: 240-253, 2006.
16. Ban K, Cooper AJ, Samuel S, Bhatti A, Patel M, Izumo S, Penninger JM, Backx PH, Oudit GY and Tsushima RG: Phosphatidylinositol 3-kinase gamma is a critical mediator of myocardial ischemic and adenosine-mediated preconditioning. Circ Res 103: 643-653, 2008.
17. Zhang CM, Gao L, Zheng YJ and Yang HT: Berbamine protects the heart from ischemia/reperfusion injury by maintaining cytosolic Ca(2+) homeostasis and preventing calpain activation. Circ J 76: 1993-2002, 2012.
18. Wu QL, Shen T, Ma H and Wang JK: Sufentanil postconditioning protects the myocardium from ischemia-reperfusion via PI3K/Akt-GSK-3β pathway. J Surg Res 178: 563-570, 2012.
19. Quintieri AM, Baldino N, Filice E, Seta L, Vitetti A, Tota B, De Cindio B, Cerra MC and Angelone T: Malvidin, a red wine polyphenol, modulates mammalian myocardial and coronary performance and protects the heart against ischemia/reperfusion injury. J Nutr Biochem 24: 1221-1231, 2013.
20. Miura T and Miki T: GSK-3beta, a therapeutic target for cardiomyocyte protection. Circ J 73: 1184-1192, 2009.
21. Abu-Izneid T, Rauf A, Khalil AA, Olatunde A, Khalid A, Alhumaydhi FA, Aljohani AS, Sahab Uddin M, Heydari M, Khayrullin M, *et al*: Nutritional and health beneficial properties of saffron (*Crocus sativus* L): A comprehensive review. Crit Rev Food Sci Nutr 17: 1-24, 2020.
22. Arzi L and Hoshyar R: Saffron anti-metastatic properties, ancient spice novel application. Crit Rev Food Sci Nutr 3: 1-12, 2021.
23. Maggi MA, Bisti S and Picco C: Saffron: Chemical composition and neuroprotective activity. Molecules 25: 5618, 2020.
24. Su X, Yuan C, Wang L, Chen R, Li X, Zhang Y, Liu C, Liu X, Liang W and Xing Y: The beneficial effects of saffron extract on potential oxidative stress in cardiovascular diseases. Oxid Med Cell Longev 2021: 6699821, 2021.
25. Rameshrad M, Razavi BM and Hosseinzadeh H: Saffron and its derivatives, crocin, crocetin and safranal: A patent review. Expert Opin Ther Pat 28: 147-165, 2018.
26. Cerdá-Bernad D, Valero-Cases E, Pastor JJ and Frutos MJ: Saffron bioactives crocin, crocetin and safranal: Effect on oxidative stress and mechanisms of action. Crit Rev Food Sci Nutr 24: 1-18, 2020.
27. Forouzanfar F, Asadpour E, Hosseinzadeh H, Boroushaki MT, Adab A, Dastpeiman SH and Sadeghnia HR: Safranal protects against ischemia-induced PC12 cell injury through inhibiting oxidative stress and apoptosis. Naunyn Schmiedebergs Arch Pharmacol 394: 707-716, 2021.
28. Lambrianidou A, Koutsougianni F, Papapostolou I and Dimas K: Recent advances on the anticancer properties of saffron (*Crocus sativus* L.) and its major constituents. Molecules 26: 86, 2020.
29. Jiang X, Li Y, Feng JL, Nik Nabil WN, Wu R, Lu Y, Liu H, Xi ZC and Xu HX: Safrana l prevents prostate cancer recurrence by blocking the re-activation of quiescent cancer cells via down-regulation of S-Phase kinase-associated protein 2. Front Cell Dev Biol 8: 598620, 2020.
30. Jin W, Xue Y, Xue Y, Liang Y, Zhang Y, Zhang J, Chu X, Wang H and Guan S: Inhibitory effects of four active components in saffron on human ether-a-go-go-related gene (hERG) K^+ currents. Gen Physiol Biophys 39: 491-498, 2020.
31. Mehdizadeh R, Parizadeh MR, Khooei AR, Mehri S and Hosseinzadeh H: Cardioprotective effect of saffron extract and safranal in isoproterenol-induced myocardial infarction in wistar rats. Iran J Basic Med Sci 16: 56-63, 2013.
32. Bharti S, Golechha M, Kumari S, Siddiqui KM and Arya DS: Akt/GSK-3β/eNOS phosphorylation arbitrates safranal-induced myocardial protection against ischemia-reperfusion injury in rats. Eur J Nutr 51: 719-727, 2012.
33. Xue Y, Jin W, Xue Y, Zhang Y, Wang H, Zhang Y, Guan S, Chu X and Zhang J: Safranal, an active constituent of saffron, ameliorates myocardial ischemia via reduction of oxidative stress and regulation of Ca^{2+} homeostasis. J Pharmacol Sci 143: 156-164, 2020.
34. Kooy NW, Royall JA and Ischiropoulos H: Oxidation of 2',7'-dichlorofluorescin by peroxynitrite. Free Radic Res 27: 245-254, 1997.
35. Sivandzade F, Bhalerao A and Cucullo L: Analysis of the mitochondrial membrane potential using the cationic JC-1 dye as a sensitive fluorescent probe. Bio Protoc 9: e3128, 2019.
36. Cui H, Miao S, Esworthy T, Zhou X, Lee SJ, Liu C, Yu ZX, Fisher JP, Mohiuddin M and Zhang LG: 3D bioprinting for cardiovascular regeneration and pharmacology. Adv Drug Deliv Rev 132: 252-269, 2018.
37. Virani SS, Alonso A, Benjamin EJ, Bittencourt MS, Callaway CW, Carson AP, Chamberlain AM, Chang AR, Cheng S, Delling FN, *et al*; American Heart Association Council on Epidemiology and Prevention Statistics Committee and Stroke Statistics Subcommittee: Heart disease and stroke statistics-2020 Update: A report from the American Heart Association. Circulation 141: e139-e596, 2020.
38. Simon-Yarza T, Bataille I and Letourneur D: Cardiovascular Bio-Engineering: Current State of the Art. J Cardiovasc Transl Res 10: 180-193, 2017.
39. Pang Z, Wang T, Li Y, Wang L, Yang J, Dong H and Li S: Liraglutide ameliorates COCl2-induced oxidative stress and apoptosis in H9C2 cells via regulating cell autophagy. Exp Ther Med 19: 3716-3722, 2020.

40. Fang Z, Luo W and Luo Y: Protective effect of α-mangostin against $CoCl_2$-induced apoptosis by suppressing oxidative stress in H9C2 rat cardiomyoblasts. Mol Med Rep 17: 6697-6704, 2018.
41. Yang Z, Yang C, Xiao L, Liao X, Lan A, Wang X, Guo R, Chen P, Hu C and Feng J: Novel insights into the role of HSP90 in cyto-protection of H2S against chemical hypoxia-induced injury in H9c2 cardiac myocytes. Int J Mol Med 28: 397-403, 2011.
42. Muñoz-Sánchez J and Chánez-Cárdenas ME: The use of cobalt chloride as a chemical hypoxia model. J Appl Toxicol 39: 556-570, 2019.
43. Xiao L, Lan A, Mo L, Xu W, Jiang N, Hu F, Feng J and Zhang C: Hydrogen sulfide protects PC12 cells against reactive oxygen species and extracellular signal-regulated kinase 1/2-mediated downregulation of glutamate transporter-1 expression induced by chemical hypoxia. Int J Mol Med 30: 1126-1132, 2012.
44. Hescheler J, Meyer R, Plant S, Krautwurst D, Rosenthal W and Schultz G: Morphological, biochemical, and electrophysiological characterization of a clonal cell (H9c2) line from rat heart. Circ Res 69: 1476-1486, 1991.
45. Goyal SN, Arora S, Sharma AK, Joshi S, Ray R, Bhatia J, Kumari S and Arya DS: Preventive effect of crocin of *Crocus sativus* on hemodynamic, biochemical, histopathological and ultrastuctural alterations in isoproterenol-induced cardiotoxicity in rats. Phytomedicine 17: 227-232, 2010.
46. Muders F, Neubauer S, Luchner A, Fredersdorf S, Ickenstein G, Riegger GA, Horn M and Elsner D: Alterations in myocardial creatinine kinase (CK) and lactate dehydrogenase (LDH) isoenzyme-distribution in a model of left ventricular dysfunction. Eur J Heart Fail 3: 1-5, 2001.
47. Amani M, Jeddi S, Ahmadiasl N, Usefzade N and Zaman J: Effect of HEMADO on level of CK-MB and LDH enzymes after ischemia/reperfusion injury in isolated rat heart. Bioimpacts 3: 101-104, 2013.
48. Ding M, Li M, Zhang EM and Yang HL: FULLEROL alleviates myocardial ischemia-reperfusion injury by reducing inflammation and oxidative stress in cardiomyocytes via activating the Nrf2/HO-1 signaling pathway. Eur Rev Med Pharmacol Sci 24: 9665-9674, 2020.
49. Madungwe NB, Zilberstein NF, Feng Y and Bopassa JC: Critical role of mitochondrial ROS is dependent on their site of production on the electron transport chain in ischemic heart. Am J Cardiovasc Dis 6: 93-108, 2016.
50. Del Rio D, Stewart AJ and Pellegrini N: A review of recent studies on malondialdehyde as toxic molecule and biological marker of oxidative stress. Nutr Metab Cardiovasc Dis 15: 316-328, 2005.
51. Giordano FJ: Oxygen, oxidative stress, hypoxia, and heart failure. J Clin Invest 115: 500-508, 2005.
52. Ghadrdoost B, Vafaei AA, Rashidy-Pour A, Hajisoltani R, Bandegi AR, Motamedi F, Haghighi S, Sameni HR and Pahlvan S: Protective effects of saffron extract and its active constituent crocin against oxidative stress and spatial learning and memory deficits induced by chronic stress in rats. Eur J Pharmacol 667: 222-229, 2011.
53. Rahaiee S, Moini S, Hashemi M and Shojaosadati SA: Evaluation of antioxidant activities of bioactive compounds and various extracts obtained from saffron (*Crocus sativus* L.): A review. J Food Sci Technol 52: 1881-1888, 2015.
54. Assimopoulou AN, Sinakos Z and Papageorgiou VP: Radical scavenging activity of *Crocus sativus* L. extract and its bioactive constituents. Phytother Res 19: 997-1000, 2005.
55. Ong SB, Samangouei P, Kalkhoran SB and Hausenloy DJ: The mitochondrial permeability transition pore and its role in myocardial ischemia reperfusion injury. J Mol Cell Cardiol 78: 23-34, 2015.
56. Ertracht O, Malka A, Atar S and Binah O: The mitochondria as a target for cardioprotection in acute myocardial ischemia. Pharmacol Ther 142: 33-40, 2014.
57. Weiss JN, Korge P, Honda HM and Ping P: Role of the mitochondrial permeability transition in myocardial disease. Circ Res 93: 292-301, 2003.
58. Park SS, Zhao H, Mueller RA and Xu Z: Bradykinin prevents reperfusion injury by targeting mitochondrial permeability transition pore through glycogen synthase kinase 3beta. J Mol Cell Cardiol 40: 708-716, 2006.
59. McCully JD, Wakiyama H, Hsieh YJ, Jones M and Levitsky S: Differential contribution of necrosis and apoptosis in myocardial ischemia-reperfusion injury. Am J Physiol Heart Circ Physiol 286: H1923-H1935, 2004.
60. Yu P, Ma S, Dai X and Cao F: Elabela alleviates myocardial ischemia reperfusion-induced apoptosis, fibrosis and mitochondrial dysfunction through PI3K/AKT signaling. Am J Transl Res 12: 4467-4477, 2020.
61. Tao J, Abudoukelimu M, Ma YT, Yang YN, Li XM, Chen BD, Liu F, He CH and Li HY: Secreted frizzled related protein 1 protects H9C2 cells from hypoxia/re-oxygenation injury by blocking the Wnt signaling pathway. Lipids Health Dis 15: 72, 2016.
62. Li HW and Xiao FY: Effect of hydrogen sulfide on cardiomyocyte apoptosis in rats with myocardial ischemia-reperfusion injury via the JNK signaling pathway. Eur Rev Med Pharmacol Sci 24: 2054-2061, 2020.
63. Dong JW, Zhu HF, Zhu WZ, Ding HL, Ma TM and Zhou ZN: Intermittent hypoxia attenuates ischemia/reperfusion induced apoptosis in cardiac myocytes via regulating Bcl-2/Bax expression. Cell Res 13: 385-391, 2003.
64. Jayanthi S, Deng X, Bordelon M, McCoy MT and Cadet JL: Methamphetamine causes differential regulation of pro-death and anti-death Bcl-2 genes in the mouse neocortex. FASEB J 15: 1745-1752, 2001.
65. Zhou T, Guo S, Wang S, Li Q and Zhang M: Protective effect of sevoflurane on myocardial ischemia-reperfusion injury in rat hearts and its impact on HIF-1α and caspase-3 expression. Exp Ther Med 14: 4307-4311, 2017.
66. Wang J, Liu J, Xie L, Cai X, Ma X and Gong J: Bisoprolol, a β1 antagonist, protects myocardial cells from ischemia-reperfusion injury via PI3K/AKT/GSK3β pathway. Fundam Clin Pharmacol 34: 708-720, 2020.
67. Maulik A, Davidson SM, Piotrowska I, Walker M and Yellon DM: Ischaemic preconditioning protects cardiomyocytes from anthracycline-induced toxicity via the PI3K pathway. Cardiovasc Drugs Ther 32: 245-253, 2018.
68. Wu X, Kihara T, Akaike A, Niidome T and Sugimoto H: PI3K/Akt/mTOR signaling regulates glutamate transporter 1 in astrocytes. Biochem Biophys Res Commun 393: 514-518, 2010.
69. Wang MY, Meng M, Yang CC, Zhang L, Li YL, Zhang L and Li L: Cornel iridoid glycoside improves cognitive impairment induced by chronic cerebral hypoperfusion via activating PI3K/Akt/GSK-3β/CREB pathway in rats. Behav Brain Res 379: 112319, 2020.
70. Thirunavukkarasu M, Selvaraju V, Tapias L, Sanchez JA, Palesty JA and Maulik N: Protective effects of *Phyllanthus emblica* against myocardial ischemia-reperfusion injury: The role of PI3-kinase/glycogen synthase kinase 3β/β-catenin pathway. J Physiol Biochem 71: 623-633, 2015.
71. Wang D, Zhang X, Li D, Hao W, Meng F, Wang B, Han J and Zheng Q: Kaempferide protects against myocardial ischemia/reperfusion injury through activation of the PI3K/Akt/GSK-3beta pathway. Mediators Inflamm 2017: 5278218, 2017.